

Original Article

Brain Effective Connectivity Pattern Modulation by Repeating Blocks of an fMRI Task

Arash Zare Sadeghi^{1,2}, Amir Homayoun Jafari³, Seyed Amir Hossein Batouli², Mohammad Ali Oghabian^{2,3*}

1- Skull Base Research Center, Iran University of Medical Sciences, Tehran, Iran.

2- Neuroimaging and Analysis Group, Imam Khomeini Hospital Complex, Tehran University of Medical sciences, Tehran, Iran.

3- Medical Physics and Biomedical Engineering Department, School of Medicine, Tehran University of Medical Sciences, Tehran Iran.

Received: 31 September 2016

Accepted: 14 November 2016

Key Words:

Dynamic Causal Modeling,

fMRI,

Sliding Window,

Time Variability.

ABSTRACT

Purpose- Effective connectivity is an active time-variable type of association between brain regions. The change of links' strength in effective connectivity networks has been studied before but as far as we know, the change in the structure of the network has not yet been tested.

Procedures- We simulated a time-variable data including three regions and one input to validate our method. In addition, we used a real fMRI data in order to evaluate the time-variability of brain effective connectivity between four brain regions using Dynamic Causal Modeling. The model space contained 38 models, all including the four regions of ventromedial prefrontal cortex, dor-solateral prefrontal cortex, amygdala, and ventral striatum. In both data, a proper moving window algorithm was used to find the changes over time.

Results- The results of simulated data matched the simulated pattern change over time. The results of real data initially showed time-dependent changes in the strength of some of the connections between brain regions. The most valid changes happened in the input and non-linear modulatory links. The input links' strength increased and the nonlinear links' strength decreased exponentially. These results show that the pattern of effective connectivity network changes and so reporting a single network for the whole data acquisition period is not meaningful.

Conclusion- In this study, we have used a method to find the time-dependent pattern changes during an fMRI task. We have shown the links' strength change over time and accordingly the structure of the network changes.

1. Introduction

Effective connectivity in the brain is the result of an active network between different brain regions, and is an image for the real reciprocal hidden neuronal effects of different regions. In other words, this effect means the controlling power of a region (or an input) on activity (or strength) of another region (or the inter-connection link of two other regions). Different

modalities have been used so far to find and quantify the effective connectivity in the brain like Electro-Encephalogram [1], Positron Emission Tomography [2-4], and Magneto-Encephalogram [5]; however, functional Magnetic Resonance Imaging (fMRI) is the most popular method used for this exploration [6].

Different methods are introduced to quantify an

*Corresponding Author:

Mohammad Ali Oghabian, PhD

Medical Physics and Biomedical Engineering Department, School of Medicine, Tehran University of Medical Sciences, Tehran Iran.

Tel: 09121962851

Email: oghabian@sina.tums.ac.ir

effective connectivity using fMRI data. The method based on Structural Equation Modeling (SEM) supposes the fMRI time-series as steady-state observations [7, 8], and therefore it cannot consider the dynamic behavior of effective connectivity networks. Granger Causality Modeling relies on statistical independence of neuronal states [9], which is also a limitation; however this method has been used to investigate the time-variability of effective connectivity networks [10-14], in other neuroimaging modalities. Dynamic Causal Modeling (DCM) is another method to find and quantify the effective connectivity networks [15]. This method finds a state-space relation which fits to the observed data, and seems to have applicability in exploring time-variability in the structure of brain effective connectivity network [16, 17].

It has been illustrated previously that an effective connectivity network is time-variable in links' strength [2, 18-20]. As a result, in this study, we aimed to test our hypothesis on the applicability of DCM for exploring the time-variability of brain effective connectivity. For this purpose, we first simulated a time-variable network with three regions and one input and in the next step we used a real fMRI data for the face validity check. For the real data [21] we selected four regions of interest: Amygdala, Ventro-medial prefrontal cortex, Dorso-lateral prefrontal cortex, and Ventral striatum according to the specific cognitive task and previous studies {Bechara, 1999 #29} [22-25]. To test the hypothesis, a sliding window approach was introduced, which to the best of our knowledge has not been tested previously in DCM for fMRI.

2. Methods

2.1. Simulated Data

We have simulated a three regions network with one input. The main structure of the network and the links' strength are depicted in Figure 1.

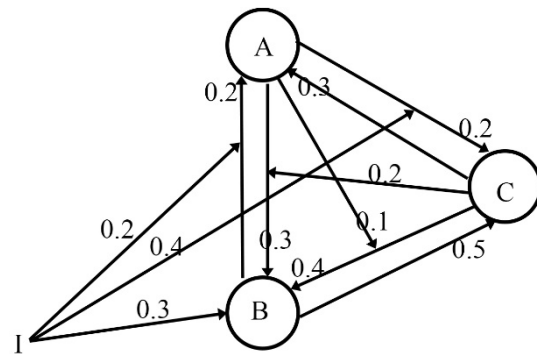


Figure 1. The structure of the simulated network for creating data. A, B, and C are three regions and I is the network's input. The numbers on the links are the time-invariable links' strength.

The input pattern was an on/off sequence which was convolved with a sample hemodynamic response and next by using the inverse of the balloon model [26] the representative time-series of neuronal population was calculated. The length of input was 960 seconds with 20 rest and act blocks; starting with rest and each for 24 seconds period. We selected the activation functions of the regions to be a simple ramp with the addition of a Gaussian noise $N(0, \sigma)$ in which σ was chosen to be 0.1, 0.2, and 0.3 for the regions A, B, and C, correspondingly. We excluded four links and let other links' strength to change over time in accordance with a pattern shown in Figure 2.

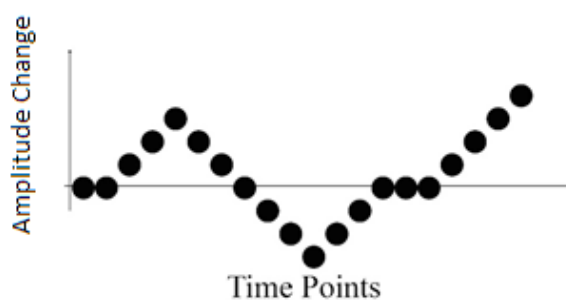


Figure 2. The pattern of links' time-variability.

The resulted time-series of the regions were assumed to be the neuronal level responses and we then implemented the forward balloon model to reach the time-series for hemodynamic level. We then assumed the TR to be three seconds and sample the time-series with frequency 1/3 Hz to reach a similar data to real fMRI. This made the total time points to be 320.

2.2. Real fMRI Data

2.2.1. Participants

The data we have used were from a previous study [21]. The control group of the original data was used in our study. This group contained 20 healthy male participants, 20-35 years old and right handed.

2.2.2. fMRI Task

The fMRI task of the source study had a blocked-design including 6 runs. Each run itself included two blocks of rest and two blocks of acts. In the first act block the images, not related to the target study, were shown to the subject and in the second act block the related images were shown. The duration of each block was chosen to be equally 24 seconds so the total run duration was 96 seconds and the approximate task duration was 10 minutes. A T1-weighted scan was performed with the following settings: matrix size: 256*256*192 mm, voxel size: 1 mm³, TE=3.55 ms, TR=1910 ms. The functional images (Echo Planar Protocol) were acquired with: TR=3000 ms, TE= 50 ms, matrix size of 64*64*192 mm, and voxel size 3 mm³.

2.3. Dynamic Causal Modeling

DCM is a method for deducing hidden neuronal states from brain activity measurements. It gives us an estimate of effective strength between neuronal populations and their modulation [27], the method was introduced for fMRI by Friston *et al.* [6, 28].

In DCM four connectivity matrices must be estimated; which their dimensions rely on the number of regions and inputs. These are the matrix A which is representative of intra-regional relations in the absence of any input, the matrix B which is the representative of inputs' effects on the links from the matrix A, matrix C which is the representative of inputs' effects on the regions, and matrix D which is the representative of regions' effects on the links from the matrix A [29]. The relation between these is as Equation 1:

$$\dot{z} = f(z, u, \theta) = Az + \left\{ \sum_{j=1}^m u_j B(j) + \sum_{i=1}^n z_i D(i) \right\} z + Cu \quad (1)$$

In which z is the neuronal signal, u is the input, θ is the parameters of forward model, m is the number of inputs, and n is the number of regions. The forward model [16, 26] is the model for mapping the measured fMRI signal to hidden neuronal states.

DCM uses a Bayesian parameter estimation framework. This Bayesian framework predominates all steps of estimation, including the calculation of links' strength and winning model selection [6, 28]. This framework needs an established knowledge to define the model space. The knowledge comes from anatomical information, functional connectivity networks, DTI data [30], or pre-published works. After defining the model space, parameter estimation process would be performed for all the models.

The estimation of the parameters of each model needs a certain amount of data as inputs, which are the Blood Oxygenation Level Dependent Signal. The number of time points in the time-series can have a direct effect on estimation of DCM networks [31].

2.3.1. DCM for Simulated Data

The three simulated time-series and the input pattern were used for specifying the DCM network and the only step needed was to estimate this network. The DCM12 algorithm was used to quantify the single time-invariable DCM network.

2.3.2. DCM for Real Data

2.3.2.1. Preprocessing

The data were preprocessed using FSL5 [32]. A correction for head motion and slice timing correction with interleaved order were implemented. A temporal filter to remove signal trend was performed. The data were intensity-normalized and registered to the standard space using affine registration. These preprocessed data were used as inputs for SPM12 first level analysis (www.fil.ion.ucl.ac.uk/spm).

2.3.2.2. DCM Calculation

Thirty eight models were entered to the model space, which included both linear and nonlinear models, and all models were estimated for each subject. We divided the models into linear and nonlinear families and by implementing Bayesian Model Selection (BMS), non-linear models showed a slightly better exceedance probability. Later, the Bayesian model averaging (BMA) was implemented on the winning family, which resulted the final network. This model was used as the input to the time-variability analysis.

2.4. Time-Variability Analysis

To quantify the time variability, we proposed a sliding window method, in which the window was moved one block in each step, and DCM was calculated each time the window was moved. The window size was selected to be in the length of two blocks and it moved one block in each step.

2.4.1. Simulated Data

Implementing the sliding window method on the three time-series, resulted in 19 DCM networks. The structure of the network was not changed and only the parameters were estimated. Eleven parameters needed to be estimated and we chose the size of two blocks to assure the convergence of the DCM algorithm as 32 data points were in two blocks of data. There were only one data and one model and so BMS/BMA algorithm were not needed.

2.4.2. Real Data

Implementing the sliding window on real data resulted in 5 DCM networks for each subject. The most complex network had one input and four regions with all possible connections, in which 60 parameters had to be estimated and with two blocks' length 64 data points were used in the estimation process. We used a single DCM model structure and followed the changes in the links' strength with time (the 5 models resulted from window movement). Since the network structure is the same for all subjects, we could use the Bayesian model averaging for reaching the final DCM within each window. This is summarized in Figure 3.

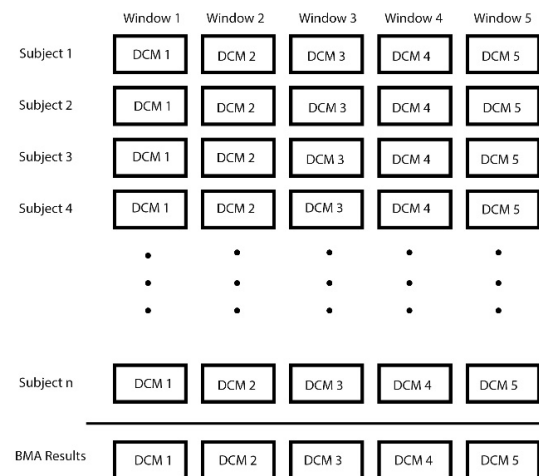


Figure 3. The scheme of method for finding group time variability. Data from subjects 1-n are windowed and in each window a Dynamic Causal Model is calculated. In the next step the Bayesian Model Averaging algorithm is implemented on these results.

3. Results

3.1. Classical DCM

3.1.1. Simulated data

Implementing classic DCM on the simulated data resulted in a network which is depicted in Figure 4.

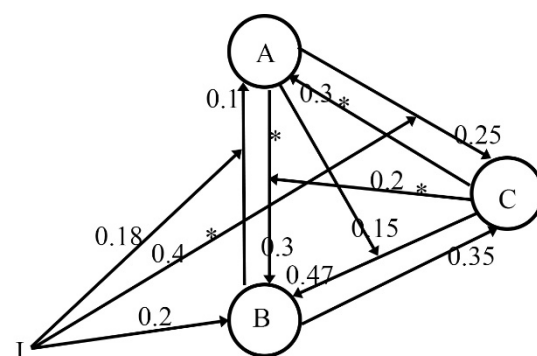


Figure 4. The result of classic DCM implementation on the simulated time-variable network. The links with star are not time-variable.

It is obvious that the four time-invariable links (shown with stars) have been estimated correctly but other links' strength differ from the original network.

3.1.2. Real Data

As mentioned above, the defined model space included 38 models. The models were defined to cover all possible networks related to the task, with the four regions of interest mentioned above. These models were estimated for all subjects.

We have divided the model space into two families. The models with any nonlinear link were added to the nonlinear family and the other models were called linear. Comparing these two families, using BMS, showed a slightly better fitness of the nonlinear models; the numbers were 0.45 for linear and 0.55 for nonlinear, even though there was not any actual dominance between families. The final network were calculated using BMA algorithm on the BMS results and it is illustrated in Figure 5.

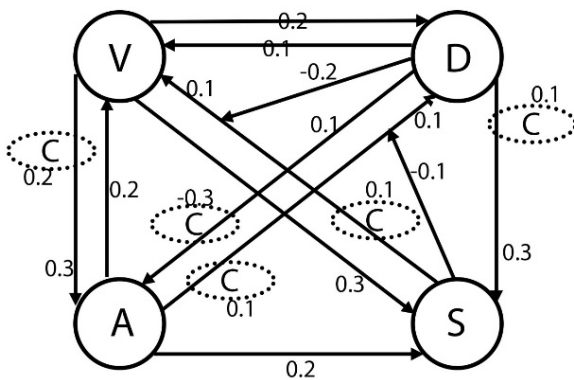


Figure 5. The final network structure. V: VMPFC, D: DLPFC, A: amygdala, and S: ventral striatum. This is the result of classic DCM. The network can be accounted as the average network over time. The dotted ellipse is the modulatory effect of input on the links. The strength of the input modulatory effect is shown near the ellipse.

There were two nonlinear effects in the network. A DLPFC effect to the link from ventral striatum to VMPFC and a ventral striatum effect to the link from amygdala to DLPFC. The input modulatory effects are shown as dotted ellipse on the relative links in the figure. As observed, five links were affected from input. In addition, ventral striatum had only one output to VMPFC region and no other regions were affected from it.

3.2. Time-Variability Analysis

3.2.1. Simulated Data

Seven links' strength were time-variable in the

network and nineteen DCMs were calculated in each time points. The resulted links' strength are shown in the Figure 6.

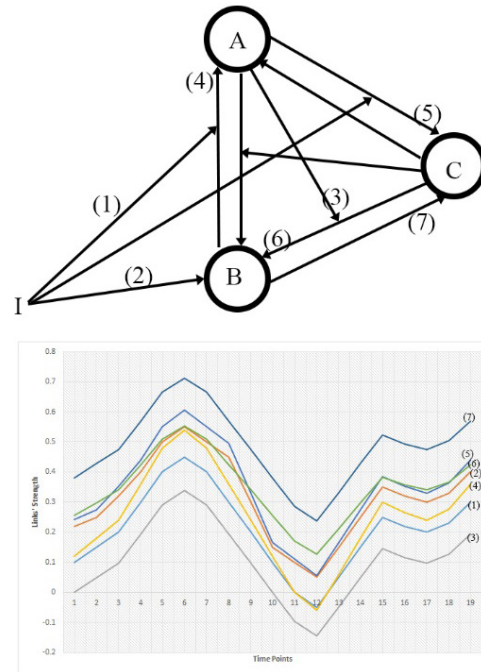


Figure 6. The time-variable change in the seven links of the simulated network is shown in this figure. The top is the structure of the network with numbers on the time-variable links. The bottom panel shows the change outcome in the links' strength.

3.2.2. Real Data

The final network outcome from the last step was used for time-variability test. The links' strength investigation showed an exponential increase in the cognitive inputs modulatory effect. The input modulatory effect on the link from DLPFC to ventral striatum grew exponentially. It started from a negative value, near zero, and increased to approximately 0.1 (Figure 7a). The same scenario happened for the input effect on the link from amygdala to DLPFC (Figure 7b). However, the input effect on the link from DLPFC to amygdala started from a negative value (-0.24), and the magnitude of this link increased later on (-0.5) (Figure 7c). The effects on the links from VMPFC to amygdala and from ventral striatum to VMPFC both started from around zero, but increased with different time constants and reached 0.21 and 0.12, respectively (Figure 7d & 7e).

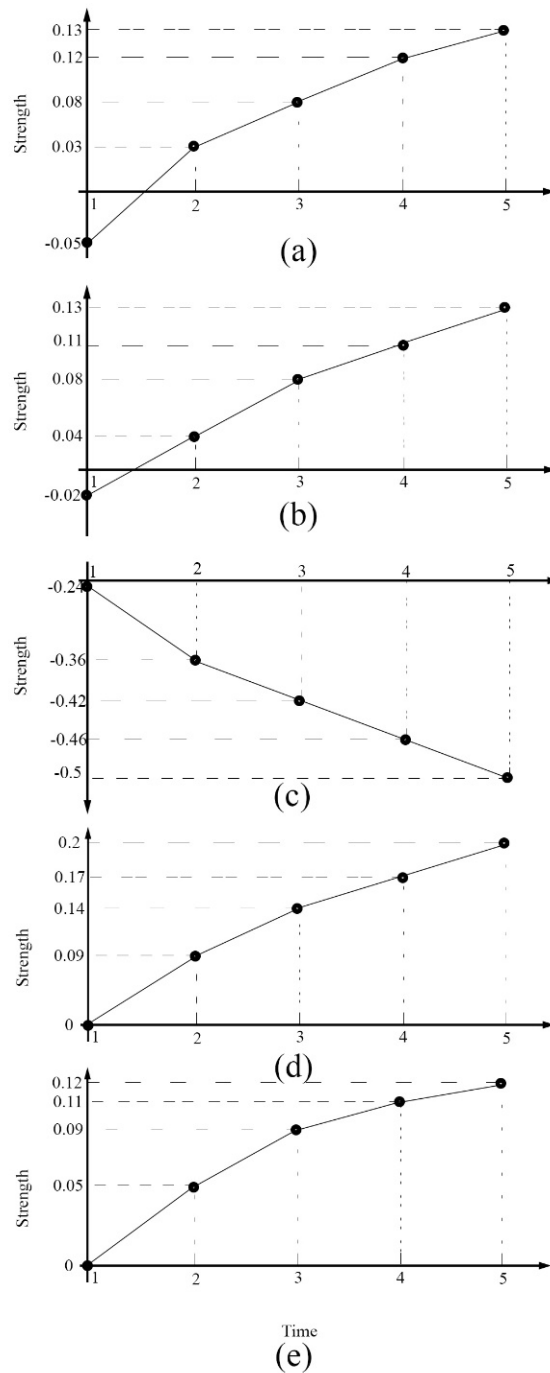


Figure 7. Time variability results. This figure shows the input modulatory effect changes over time. The effect change on the link from DLPFC to ventral striatum (a), the effect change on the link from amygdala to DLPFC (b), the effect change on the link from DLPFC to amygdala (c), the effect change on the link from VMPFC to amygdala (d), and the effect change on the link from ventral striatum to VMPFC (e).

The effect of ventral striatum to the link from amygdala to DLPFC began from a negative value of -0.15 and exponentially increased to -0.06 (Figure 8a). The effect of DLPFC on the link from ventral

striatum to VMPFC also began from a negative value of -0.4 and increased to -0.02 (Figure 8b), but the initial magnitude of this effect was about three times larger than the other nonlinear effects.

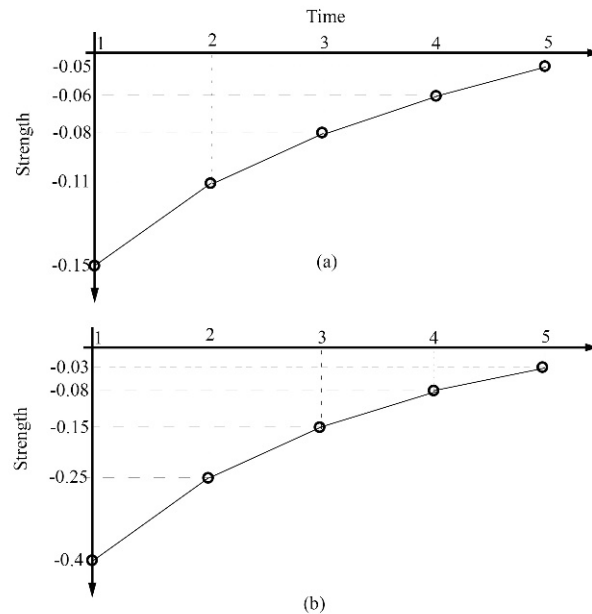


Figure 8. Time variability results in the model space. The change of nonlinear links are shown in this figure. The effect change of ventral striatum on the link from amygdala to DLPFC (a), and the effect change of DLPFC on the link from ventral striatum to VMPFC.

Tracking the parameter changes in time revealed that the final structure of the network changed (Figure 9). As it is shown in the first time point, the only input modulatory effect was the effect on the link from DLPFC to amygdala. The other input

modulatory effects gradually appeared over time. On the other hand, the nonlinear links existed at the beginning of the imaging, but they disappeared at the end.

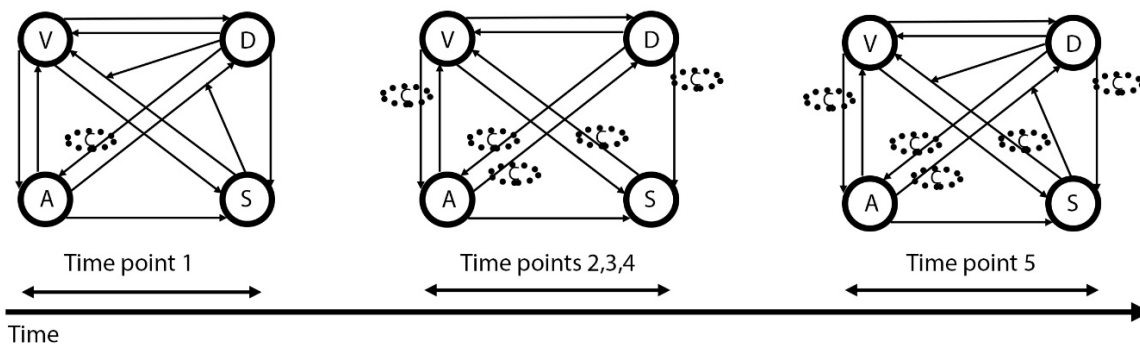


Figure 9. The network structure evolution over time. This figure shows the structure change in 5 time points. The time points 2,3, and 4 have the same structure but different parameter values.

4. Discussion

In this paper, using a simulated network data and a real data from an older fMRI study on a cognitive task comprising normal subjects, we initially tested a classical Dynamic Causal Model on the data to explore the effective connectivity network between the regions. The DCM network outcome

for real data was later used for the time-variability analysis. The time-variability was tested with a two blocks length moving window which moved for one block in each step. The parameters of the simulated network was re-estimated each time the window moved, resulting 19 DCM networks. For the real data, the DCM network from the classic DCM calculation were re-estimated each time the

window was moved. Therefore, 5 DCMs were quantified for each subject, and consequently, using BMA, 5 group DCMs were calculated.

The regions of interest in the real data were ventro-medial prefrontal cortex, dorso-lateral prefrontal cortex, amygdala, and ventral striatum. Calculating DCM among these regions in our data resulted in a network with two nonlinear effects emerging from DLPFC and ventral striatum to the link from ventral striatum to VMPFC, and from amygdala to DLPFC. Five links were affected from the cognitive input, including the links from DLPFC to ventral striatum, ventral striatum to VMPFC, amygdala to DLPFC, DLPFC to amygdala, and VMPFC to amygdala. VMPFC, DLPFC, and amygdala were all reciprocally connected. Ventral striatum had inputs from these three regions but had only one output to VMPFC.

The DCM network outcome for the simulated data showed that the implementation of time-invariable method on a time-variable network is not appropriate as the strength of time variable links were not estimated correctly. Using time-variable method showed a good fit to the links' strength pattern change over time. For the real data, the time-variability test showed changes in the strength of few of the links among the 5 DCMs, which had exponential forms. The magnitude of the input modulatory effects showed increment, and that of the nonlinear effects showed decrement. By omitting the links with zero strength, the change in the structure of the network was revealed.

As stated above, time-variability in effective connectivity has been studied previously in other modalities, but it is rarely studied in DCM for fMRI [31]. Friston and colleagues, using a Hebbian model for the PET data in twelve consecutive measurements showed that effective connectivity grew stronger in correlation with the task [2]. Havlicek and colleagues used Kalman filter as a time-variable model to estimate the Granger causality changes with time on a simulated data and two real fMRI data, and showed the superiority of time-variant models on time-invariant models [10]. Plomp and colleagues, using a multivariate time-varying Granger causality method on epileptic EEG data, showed changes in the connections between brain lobes with time [11]. Similarly, the changes in the GCM parameters in

brain during measurements has been illustrated in many previous works [12, 13]. The changes in DCM network over time for MEG data is also observed previously [33].

The brain has been shown to have temporal dynamicity and therefore exploring time-variability in brain connectivity networks is advantageous for understanding the real-time behavior of the brain. In fact, EEG or fMRI data in essence are time-variable, and therefore their analysis methods should always consider the time-variable nature of the signals [15, 17].

In this study, we investigated the applicability of using DCM analysis to explore the time-variability of brain effective connectivity. For this purpose, we used a sliding-window method which to the best of our knowledge has not been previously used in DCM for fMRI. The benefit of using a sliding window method is that we did not interfere in original DCM estimation process. The results showed that the brain regions would be effectively connected, the connection which may change and disappear/appear with time. The results also showed that using a classic time-invariable DCM for a time-variable network concludes wrong estimations. Despite the strength, this study was limited in choosing a good step size as one whole block. The step size can be chosen to be as short as TR but the estimation process must be changed. The other issue was limiting the time-variability analysis to a single structure; however, this resulted in a single reliable time-variable DCM network for the whole group, but defining the model space for each 5 DCM estimation could lead to a different outcome. The other issue relating to the simulation was using a single structure for the model and if the model space included more models BMS/BMA algorithms could be implemented on the results.

References

- 1- L. Astolfi, F. Cincotti, D. Mattia, S. Salinari, C. Babiloni, A. Basilisco, et al., "Estimation of the effective and functional human cortical connectivity with structural equation modeling and directed transfer function applied to high-resolution EEG," *Magn Reson Imaging*, vol. 22, pp. 1457-70, Dec 2004.
- 2- K. J. Friston, C. D. Frith, and R. S. J. Frackowiak, "Time-dependent changes in effective connectivity measured with PET," *Human Brain Mapping*, vol. 1, pp. 69-79, 1993.

- 3- F. Ferrarelli, H. M. Haraldsson, T. E. Barnhart, A. D. Roberts, T. R. Oakes, M. Massimini, et al., "A [17F]-fluoromethane PET/TMS study of effective connectivity," *Brain research bulletin*, vol. 64, pp. 103-113, 2004/08// 2004.
- 4- A. R. Laird, J. M. Robbins, K. Li, L. R. Price, M. D. Cykowski, S. Narayana, et al., "Modeling motor connectivity using TMS/PET and structural equation modeling," *NeuroImage*, vol. 41, pp. 424-436, 02/15 2008.
- 5- S. J. Kiebel, M. I. Garrido, R. Moran, C.-C. Chen, and K. J. Friston, "Dynamic causal modeling for EEG and MEG," *Human Brain Mapping*, vol. 30, pp. 1866-1876, 2009.
- 6- K. J. Friston, L. Harrison, and W. Penny, "Dynamic causal modelling," *Neuroimage*, vol. 19, pp. 1273-302, Aug 2003.
- 7- A. R. McIntosh and F. Gonzalez-Lima, "Structural equation modeling and its application to network analysis in functional brain imaging," *Human Brain Mapping*, vol. 2, pp. 2-22, 1994.
- 8- K. E. Stephan, "On the role of general system theory for functional neuroimaging," *Journal of Anatomy*, vol. 205, pp. 443-470, 10/11/accepted 2004.
- 9- X. Wen, G. Rangarajan, and M. Ding, "Is Granger Causality a Viable Technique for Analyzing fMRI Data?," *PLoS ONE*, vol. 8, p. e67428, 2013.
- 10- M. Havlicek, J. Jan, M. Brazdil, and V. D. Calhoun, "Dynamic Granger causality based on Kalman filter for evaluation of functional network connectivity in fMRI data," *NeuroImage*, vol. 53, pp. 65-77, 10/15/ 2010.
- 11- G. Plomp, R. Tyrand, L. Astolfi, B. He, M. Seeck, C. M. Michel, et al., "3. Dynamic effective connectivity of epileptic networks determined with high density EEG source analysis," *Clinical Neurophysiology*, vol. 123, p. e109, 10// 2012.
- 12- J. Toppi, F. Babiloni, G. Vecchiato, F. De Vico Fallani, D. Mattia, S. Salinari, et al., "Towards the time varying estimation of complex brain connectivity networks by means of a General Linear Kalman Filter approach," *Conf Proc IEEE Eng Med Biol Soc*, vol. 2012, pp. 6192-5, 2012.
- 13- L. Astolfi, J. Toppi, G. Wood, S. Kober, M. Risetti, L. Macchiusi, et al., "Advanced methods for time-varying effective connectivity estimation in memory processes," *Conf Proc IEEE Eng Med Biol Soc*, vol. 2013, pp. 2936-9, 2013.
- 14- J. Toppi, D. Mattia, A. Anzolin, M. Risetti, M. Petti, F. Cincotti, et al., "Time varying effective connectivity for describing brain network changes induced by a memory rehabilitation treatment," *Conf Proc IEEE Eng Med Biol Soc*, vol. 2014, pp. 6786-9, 2014.
- 15- A. Zare Sadeghi, A. H. Jafari, M. A. Oghabian, H. R. Salighehrad, S. A. H. Batouli, S. Raminfar, et al., "Changes in Effective Connectivity Network Patterns in Drug Abusers, Treated With Different Methods," *Basic and Clinical Neuroscience Journal*, vol. 8, pp. 285-298, 2017.
- 16- K. J. Friston, A. Mechelli, R. Turner, and C. J. Price, "Nonlinear responses in fMRI: the Balloon model, Volterra kernels, and other hemodynamics," *Neuroimage*, vol. 12, pp. 466-77, Oct 2000.
- 17- A. Zare-Sadeghi, A. Jafari, M. Oghabian, H. Salighe-Rad, and S. Batouli, "Pattern Change of Inhibitory Drug Craving Control in Brain: A Study of Effective Connectivity," *Journal of Biomedical Physics and Engineering*, 2017.
- 18- M. Ding, S. L. Bressler, W. Yang, and H. Liang, "Short-window spectral analysis of cortical event-related potentials by adaptive multivariate autoregressive modeling: data preprocessing, model validation, and variability assessment," *Biol Cybern*, vol. 83, pp. 35-45, Jul 2000.
- 19- J. Ginter, Jr., K. J. Blinowska, M. Kaminski, and P. J. Durka, "Phase and amplitude analysis in time-frequency space--application to voluntary finger movement," *J Neurosci Methods*, vol. 110, pp. 113-24, Sep 30 2001.
- 20- M. Kaminski, P. Szerling, and K. Blinowska, "Comparison of methods for estimation of time-varying transmission in multichannel data," in *Information Technology and Applications in Biomedicine (ITAB)*, 2010 10th IEEE International Conference on, 2010, pp. 1-4.
- 21- H. Tabatabaei-Jafari, H. Ekhtiari, H. Ganjgahi, P. Hassani-Abharian, M. A. Oghabian, A. Moradi, et al., "Patterns of brain activation during craving in heroin dependents successfully treated by methadone maintenance and abstinence-based treatments," *J Addict Med*, vol. 8, pp. 123-9, Mar-Apr 2014.
- 22- A. Bechara, H. Damasio, A. R. Damasio, and G. P. Lee, "Different contributions of the human amygdala and ventromedial prefrontal cortex to decision-making," *The Journal of Neuroscience*, vol. 19, pp. 5473-5481, 1999.
- 23- A. Bechara, S. Dolan, N. Denburg, A. Hindes, S. W. Anderson, and P. E. Nathan, "Decision-making deficits, linked to a dysfunctional ventromedial

prefrontal cortex, revealed in alcohol and stimulant abusers," *Neuropsychologia*, vol. 39, pp. 376-389, 2001.

24- A. Bechara, "Decision making, impulse control and loss of willpower to resist drugs: a neurocognitive perspective," *Nature neuroscience*, vol. 8, pp. 1458-1463, 2005.

25- X. Noël, M. Van Der Linden, and A. Bechara, "The Neurocognitive Mechanisms of Decision-making, Impulse Control, and Loss of Willpower to Resist Drugs," *Psychiatry (Edgmont)*, vol. 3, pp. 30-41, 05/2006.

26- R. B. Buxton, E. C. Wong, and L. R. Frank, "Dynamics of blood flow and oxygenation changes during brain activation: the balloon model," *Magn Reson Med*, vol. 39, pp. 855-64, Jun 1998.

27- K. E. Stephan, W. D. Penny, J. Daunizeau, R. J. Moran, and K. J. Friston, "Bayesian Model Selection for Group Studies," *NeuroImage*, vol. 46, pp. 1004-1017, 03/20 2009.

28- K. E. Stephan, L. M. Harrison, S. J. Kiebel, O. David, W. D. Penny, and K. J. Friston, "Dynamic causal models of neural system dynamics: current state and future extensions," *J Biosci*, vol. 32, pp. 129-44, Jan 2007.

29- K. E. Stephan, L. Kasper, L. M. Harrison, J. Daunizeau, H. E. M. den Ouden, M. Breakspear, et al., "Nonlinear Dynamic Causal Models for fMRI," *NeuroImage*, vol. 42, pp. 649-662, 05/11 2008.

30- K. E. Stephan, M. Tittgemeyer, T. R. Knösche, R. J. Moran, and K. J. Friston, "Tractography-based priors for dynamic causal models," *Neuroimage*, vol. 47, pp. 1628-1638.

31- K. J. Friston, J. Kahan, B. Biswal, and A. Razi, "A DCM for resting state fMRI," *Neuroimage*, vol. 94, pp. 396-407, 12/09/accepted 2014.

32- M. Jenkinson, C. F. Beckmann, T. E. Behrens, M. W. Woolrich, and S. M. Smith, "FSL," *Neuroimage*, vol. 62, pp. 782-90, Aug 15 2012.

33- C. Poch, M. I. Garrido, J. M. Igoa, M. Belinchon, I. Garcia-Morales, and P. Campo, "Time-varying effective connectivity during visual object naming as a function of semantic demands," *J Neurosci*, vol. 35, pp. 8768-76, Jun 10 2015.